Curvature statistics of some few-body Debye-Huckel and Lennard-Jones systems

1980 J. Phys. A: Math. Gen. 13 833

(http://iopscience.iop.org/0305-4470/13/3/017)

J. Phys. A: Math. Gen. **13** (1980) 833–854. Printed in Great Britain

Curvature statistics of some few-body Debye–Hückel and Lennard–Jones systems

J F C van Velsen†

Department of Physics, Ahmadu Bello University, Zaria, Nigeria

Received 11 January 1979, in final form 2 July 1979

Abstract. The motion of a conservative classical system is considered as a geodesic flow on a Riemannian manifold. Expressions for various curvature tensors are derived. It is shown that the Riemann tensor of a conservative system with N degrees of freedom is defined by $\frac{1}{2}N(N-1)$ curvatures $c_{ij}(i<j)$, for which expressions and elementary properties are derived. The manifold has negative curvature if all $c_{ij}<0$. For closed manifolds negative curvature implies that the system is a K-system, but we show that one cannot have $c_{ij}<0$ everywhere in the configuration space of a conservative system.

The results are presented of numerical calculations of the curvature of 8- and 16-particle systems interacting according to the Debye–Hückel and Lennard–Jones potential. Good agreement is found between the 8- and 16-particle curvature distribution functions. In general, more than half of the c_{ij} at a given point in configuration space are negative. Negative curvature turns out to be a rare phenomenon, although it is found in more than half of the configuration space of Lennard–Jones systems at low density and energy $E=0$.

1. Introduction

Jacobi's form of Maupertuis' least-action principle is a convenient starting point for a geometrical formulation of classical mechanics (Goldstein 1950). It shows that the trajectories of a conservative system can be interpreted as geodesics on a Riemannian manifold. The metric of this manifold is a simple function of the potential and the total energy of the system. Given the metric, one can calculate the Riemann tensor, which plays a fundamental role in differential geometry.

In classical mechanics there seem to be at least two good reasons for studying the Riemann tensor of a system. Firstly, the Riemann tensor provides a picture of the local behaviour of the trajectories. This is expressed in the equation of geodesic deviation (see below, equation (4.2)). Particularly important for the few- and many-particle systems in statistical mechanics is the fact that the Riemann tensor can be obtained from the metric without having to integrate the equations of motion, for integration of the equations of motion on a macroscopic time scale should be virtually impossible if the system is to have strong ergodic properties (Balescu 1975). But, using the Riemann tensor, one can at least compute the local behaviour everywhere.

Secondly, knowledge of the Riemann tensor enables one to apply, for example, the Lobatchevsky–Hadamard theorem on the global properties of the system. This theorem (Arnol'd and Avez 1968) says that the geodesic flow on a closed manifold of

† Present address: Instituut voor Theoretische Fysica, Princetonplein 5, PO Box 80.006, 3508 TA Utrecht, The Netherlands.

0305-4470/80/030833+22$01.00

negative curvature (a property which one can verify given the Riemann tensor) is a K-system. A K-system is mixing and ergodic, which shows that calculation of the Riemann tensor could be a method of explicitly verifying ergodicity.

In this paper we would like to describe a practical method for the calculation of the Riemann tensor of a conservative system and for testing negative curvature, and to do such calculations for some systems of interest to mechanics and statistical mechanics.

In § 2 the Riemann tensor of a conservative system is calculated and reduced to a useful normal form which greatly simplifies practical computations of the Riemann tensor. Notwithstanding this reduction, a formal evaluation of the curvature expressions is feasible only for systems with a relatively small number of degrees of freedom. For larger systems the calculation of the curvature might be done numerically.

Section 3 introduces the geometric concept of sectional curvature and a particular set of sectional curvatures. The elements of this set will here be called eigencurvatures. They give a characterisation of the local properties of the trajectories. A method of calculating the eigencurvatures is described, and some of their elementary properties are deduced.

In § 4 manifolds of negative curvature and the Lobatchevsky–Hadamard theorem will be discussed, with emphasis on the implications for mechanics and ergodic theory.

After these theoretical sections we first give two simple examples, namely the Kepler and Hénon–Heiles problems. The Riemann tensor in these two-dimensional systems is a scalar which can be computed analytically. This is done in § 5. Then we turn to curvature computations in some realistic few-body systems. We shall consider systems consisting of 8 or 16 particles contained in a cube. The particles interact according to the Debye–Hückel (DH) or the Lennard–Jones (LJ) potential. The DH potential is repulsive throughout, while the LJ potential consists of an r^{-12} repulsive short-range part and an r^{-6} attractive long-range part. These systems will be considered at different densities and energies in order to determine the dependence of the curvature on these quantities. The formal expressions for the curvature clearly cannot be given (at least, they do not seem to make sense). However, we can obtain a useful picture of the behaviour of the curvature by random sampling of the configuration space. In that manner the distributions of the various curvature quantities are obtained. The method of calculation of the distributions is described in § 6.

Sections 7 and 8 describe the results of numerical work on the DH and LJ systems respectively. The different interactions and densities give rise to clearly distinguishable distributions. The curvature distribution functions are roughly the same for the 8- and 16-particle systems, apart from scale factors in the energy and curvature. In particular the distributions depend on density and energy in the same way. The theoretical predictions of §§ 3 and 4 are verified. The important case of negative curvature, representing very erratic behaviour of the trajectories, is found in more than half of the configuration space of the LJ system at $E = 0$.

In § 9 we conclude the paper with some remarks regarding this and future work on the curvature of conservative systems in classical mechanics.

2. The Riemann tensor of a conservative system

2.1. The motion of a conservative system represented as a geodesic flow

Consider a classical mechanical system with N degrees of freedom defined by the

time-independent Hamiltonian

$$H(p_1, \ldots, p_N, q^1, \ldots, q^N) = \tfrac{1}{2}\alpha^{ij} p_i p_j + V(q^1, \ldots, q^N), \tag{2.1}$$

where the matrix α^{ij} is assumed to be symmetric. The inverse of α^{ij} is denoted by α_{ij},

$$\alpha^{ij}\alpha_{jk} = \delta^i{}_k. \tag{2.2}$$

The equations of motion of the system are the Hamiltonian equations

$$\dot{q}^k = \partial H/\partial p_k, \qquad \dot{p}_k = -\partial H/\partial q^k, \qquad k = 1, \ldots, N. \tag{2.3}$$

The Hamiltonian is a constant of the motion, $\mathrm{d}H/\mathrm{d}t = 0$. For given initial conditions $p^{(0)}$, $q^{(0)}$ therefore, $H(p(t), q(t))$ is a constant:

$$H(p(t), q(t)) = H(p^{(0)}, q^{(0)}) = E, \tag{2.4}$$

the energy of the system.

On a manifold of constant energy in phase space the actual path of the system is an extremum of the integral

$$\int (E - V(q))^{1/2} (\alpha_{ij}\, \mathrm{d}q^i\, \mathrm{d}q^j)^{1/2}. \tag{2.5}$$

This proposition is Jacobi's form of the least-action principle (Goldstein 1950). Now define the path element $\mathrm{d}s$ and the metric tensor g_{ij} by

$$\mathrm{d}s^2 = (E - V(q))\alpha_{ij}\, \mathrm{d}q^i\, \mathrm{d}q^j = g_{ij}\, \mathrm{d}q^i\, \mathrm{d}q^j. \tag{2.6}$$

The inverse of g_{ij} is denoted by g^{ij},

$$g^{ij}g_{jk} = \delta^i{}_k. \tag{2.7}$$

Raising and lowering of indices are defined in the usual way, e.g. $x_i = g_{ij}x^j$.

Jacobi's form of the least-action principle can now be written as

$$\delta \int \mathrm{d}s = 0. \tag{2.8}$$

This shows that the dynamical system defined by equations (2.1), (2.3) and (2.4) is a geodesic flow on the manifold of constant energy E, with metric given by equation (2.6).

Using equations (2.2) and (2.3) the kinetic energy $T = E - V(q)$ can be written

$$T = \tfrac{1}{2}\alpha^{ij} p_i p_j = \tfrac{1}{2}\alpha_{ij}(\mathrm{d}q^i/\mathrm{d}t)(\mathrm{d}q^j/\mathrm{d}t). \tag{2.9}$$

Since the kinetic energy is positive definite, so are α_{ij} and α^{ij}. This shows that the metric is positive definite, and that it defines a positive-definite bilinear form $(\boldsymbol{x}\,.\,\boldsymbol{y})$ through

$$(\boldsymbol{x}\,.\,\boldsymbol{y}) = g_{ij}x^i y^j = x_j y^j. \tag{2.10}$$

The connection coefficients $\Gamma^i{}_{jk}$ are defined by

$$\Gamma^i{}_{jk} = \tfrac{1}{2}g^{im}(\partial g_{mj}/\partial q^k + \partial g_{mk}/\partial q^j - \partial g_{jk}/\partial q^m). \tag{2.11}$$

For this expression and for the definition of the Riemann tensor (2.17) below the reader is referred to Misner *et al* (1973). We shall also follow the sign conventions of this reference.

We now assume that α_{ij} does not depend on the coordinates $q^1, \ldots, q^N$. Upon substitution of g_{ij} from equation (2.6) Γ^i_{jk} becomes

$$\Gamma^i_{jk} = \frac{1}{2}\frac{1}{E-V}\alpha^{im}\frac{\partial V}{\partial q^m}\alpha_{jk} - \frac{1}{2}\frac{1}{E-V}\left(\delta^i{}_j\frac{\partial V}{\partial q^k} + \delta^i{}_k\frac{\partial V}{\partial q^j}\right). \tag{2.12}$$

Defining the quantities

$$\nu_i = \partial V/\partial q^i \qquad \text{and} \qquad \nu_{ij} = \partial^2 V/\partial q^i \partial q^j, \tag{2.13}$$

equation (2.12) can be written as

$$\Gamma^i_{jk} = \frac{1}{2}\frac{1}{E-V}\alpha^{im}\nu_m\alpha_{jk} - \frac{1}{2}\frac{1}{E-V}(\delta^i{}_j\nu_k + \delta^i{}_k\nu_j). \tag{2.14}$$

The equation for the geodesics can be written

$$\ddot{q}^i + \Gamma^i_{jk}\dot{q}^j\dot{q}^k = 0. \tag{2.15}$$

The dots now represent differentiation with respect to the arc-length parameter s. From equations (2.6) and (2.9) one finds the velocity along the geodesics:

$$\mathrm{d}s/\mathrm{d}t = \sqrt{2}(E - V(q)). \tag{2.16}$$

2.2. The calculation of the Riemann tensor

In terms of the connection coefficients Γ^i_{jk} the Riemann tensor $R^i{}_{jkl}$ can be written in the form

$$R^i{}_{jkl} = \partial\Gamma^i_{jl}/\partial q^k - \partial\Gamma^i_{jk}/\partial q^l + \Gamma^i_{kn}\Gamma^n_{jl} - \Gamma^i_{ln}\Gamma^n_{jk}. \tag{2.17}$$

Substitution of equation (2.14) followed by some algebra gives

$$\begin{aligned} 4(E-V)^2 R^i{}_{jkl} &= 3\alpha^{im}\nu_m(\alpha_{jl}\nu_k - \alpha_{jk}\nu_l) + 3\nu_j(\delta^i{}_k\nu_l - \delta^i{}_l\nu_k) + (\nu_m\alpha^{mn}\nu_n)(\delta^i{}_l\alpha_{jk} - \delta^i{}_k\alpha_{jl}) \\ &\quad + 2(E-V)(\alpha^{im}\nu_{mk}\alpha_{jl} - \alpha^{im}\nu_{ml}\alpha_{jk} - \delta^i{}_l\nu_{jk} + \delta^i{}_k\nu_{jl}). \end{aligned} \tag{2.18}$$

The components $R^{ij}{}_{kl}$ are found by raising the index j in $R^i{}_{jkl}$: $R^{ij}{}_{kl} = g^{jm}R^i{}_{mkl}$. With $g^{jm} = \alpha^{jm}/(E-V)$ one finds

$$\begin{aligned} 4(E-V)^3 R^{ij}{}_{kl} &= 3\alpha^{im}\nu_m(\delta^j{}_l\nu_k - \delta^j{}_k\nu_l) + 3\alpha^{jm}\nu_m(\delta^i{}_k\nu_l - \delta^i{}_l\nu_k) \\ &\quad + (\nu_m\alpha^{mn}\nu_n)(\delta^i{}_l\delta^j{}_k - \delta^i{}_k\delta^j{}_l) \\ &\quad + 2(E-V)(\delta^j{}_l\alpha^{im}\nu_{mk} - \delta^i{}_k\alpha^{im}\nu_{ml} - \delta^i{}_l\alpha^{jm}\nu_{mk} + \delta^i{}_k\alpha^{jm}\nu_{ml}). \end{aligned} \tag{2.19}$$

The Ricci tensor with mixed components is $R^i{}_k = R^{ij}{}_{kj}$. Using equation (2.19) one obtains

$$\begin{aligned} 4(E-V)^3 R^i{}_k &= \{2(E-V)(\alpha^{mn}\nu_{mn}) - (N-4)(\nu_m\alpha^{mn}\nu_n)\}\delta^i{}_k \\ &\quad + 3(N-2)\alpha^{im}\nu_m\nu_k + 2(N-2)(E-V)\alpha^{im}\nu_{mk}. \end{aligned} \tag{2.20}$$

Contracting once more gives the Riemann curvature scalar R:

$$R = \frac{N-1}{(E-V)^2}\left\{\alpha^{mn}\nu_{mn} - \frac{1}{4}\left(\frac{N-6}{E-V}\right)\nu_m\alpha^{mn}\nu_n\right\}. \tag{2.21}$$

2.3. Reduction of the Riemann tensor expressions

Since α^{ij} in equation (2.1) is real and symmetric there exists a real coordinate transformation $A^i{}_j$ which transforms α^{ij} into the unit matrix:

$$A^i{}_k A^j{}_l \alpha^{kl} = \delta_{ij}. \tag{2.22}$$

Clearly $\alpha_{ij} = \delta_{ij}$ in the new frame.

When it is assumed that the α^{ij} are independent of the coordinates $q^1, \ldots, q^N$, then the $A^i{}_j$ are constant as well. In this case the transformation laws for the ν_i and ν_{ij} are given by

$$\nu'_k = (A^{-1})^i{}_k \nu_i \qquad \text{and} \qquad \nu'_{kl} = (A^{-1})^i{}_k (A^{-1})^j{}_l \nu_{ij}. \tag{2.23}$$

Putting $\alpha_{ij} = \delta_{ij}$ in equation (2.19) and dropping the prime gives

$$\begin{aligned} 4(E-V)^3 R^{ij}{}_{kl} = {} & 3\nu_i(\delta_{jl}\nu_k - \delta_{jk}\nu_l) + 3\nu_j(\delta_{ik}\nu_l - \delta_{il}\nu_k) + (\nu_m\nu_m)(\delta_{il}\delta_{jk} - \delta_{ik}\delta_{jl}) \\ & + 2(E-V)(\delta_{jl}\nu_{ik} - \delta_{jk}\nu_{il} - \delta_{il}\nu_{jk} + \delta_{ik}\nu_{jk}). \end{aligned} \tag{2.24}$$

A special case, in which the coordinate transformation $A^i{}_j$ has a particularly simple form, is that of a system of particles with possibly different masses. The matrix α_{ij} is diagonal with the masses along the diagonal. After the transformation the kinetic energy is $T = \frac{1}{2}\Sigma p_i^2$, so that all particles can be assumed to have mass $m = 1$.

The expression (2.24) can be simplified by introducing the matrix μ_{ij} through

$$\mu_{ij} = 3\nu_i\nu_j + 2(E-V)\nu_{ij}. \tag{2.25}$$

In terms of this matrix, equation (2.24) can be written as

$$4(E-V)^3 R^{ij}{}_{kl} = \mu_{jl}\delta_{ik} + \mu_{ik}\delta_{jl} - (\nu_m\nu_m)\delta_{ik}\delta_{jl} - \{\mu_{jk}\delta_{il} + \mu_{il}\delta_{jk} - (\nu_m\nu_m)\delta_{il}\delta_{jk}\}. \tag{2.26}$$

The matrix μ_{ij} is symmetric and can therefore be diagonalised by an orthogonal coordinate transformation. Let the eigenvalues of μ_{ij} be denoted λ_i. In the new coordinates equation (2.26) becomes

$$4(E-V)^3 R^{ij}{}_{kl} = \Big(\lambda_i + \lambda_j - \sum_m \nu_m\nu_m\Big)(\delta_{ik}\delta_{jl} - \delta_{il}\delta_{jk}). \tag{2.27}$$

No summation over i and j is implied on the right-hand side. Similarly we can write the Ricci tensor in terms of μ_{ij} and its eigenvalues. From either (2.20) or (2.27) one derives

$$4(E-V)^3 R^i{}_j = (N-2)\mu_{ij} + \Big\{\mathrm{Tr}(\mu_{mn}) - (N-1)\sum_m \nu_m\nu_m\Big\}\delta_{ij} \tag{2.28a}$$

$$= \Big\{(N-1)\Big(\lambda_i - \sum_m \nu_m\nu_m\Big) + \sum_{\substack{k \\ k\neq i}} \lambda_k\Big\}\delta_{ij}. \tag{2.28b}$$

In the last expression no summation over i is implied.

Finally the Riemann scalar can be written as

$$4(E-V)^3 R = (N-1)\Big\{2\,\mathrm{Tr}(\mu_{mn}) - N\sum_m \nu_m\nu_m\Big\} \tag{2.29a}$$

$$= (N-1)\Big\{2\sum_i \lambda_i - N\sum_m \nu_m\nu_m\Big\}. \tag{2.29b}$$

For the simple two-dimensional case $N=2$ and there is only one non-vanishing independent component $R^{ij}{}_{kl}$, namely $R^{12}{}_{12}$. The Riemann scalar $R=2R^{12}{}_{12}$. If the potential is denoted $V(x, y)$ and $\alpha_{ij}=\delta_{ij}$ then equation (2.21) reduces to

$$R=\frac{1}{(E-V)^2}\left[\frac{\partial^2 V}{\partial x^2}+\frac{\partial^2 V}{\partial y^2}+\frac{1}{E-V}\left\{\left(\frac{\partial V}{\partial x}\right)^2+\left(\frac{\partial V}{\partial y}\right)^2\right\}\right]. \tag{2.30}$$

3. Sectional curvature and eigencurvatures

3.1. Definitions

Let us now proceed with the geometrical interpretation of equation (2.27). First we observe that the curvature of a Riemannian manifold can be described in terms of sectional or Gaussian curvatures. These curvatures relate to two-dimensional surfaces.

At a point Q of the manifold a pair of tangent vectors $\boldsymbol{x}$ and $\boldsymbol{y}$ spans a plane section S_Q. The sectional curvature K along the plane section is formally defined as

$$K(S_Q)=\frac{R^{ij}{}_{kl}x_i y_j x^k y^l}{(\boldsymbol{x}\cdot\boldsymbol{x})(\boldsymbol{y}\cdot\boldsymbol{y})-(\boldsymbol{x}\cdot\boldsymbol{y})^2} \tag{3.1}$$

(Helgason 1962). It follows from this definition that K is an invariant, i.e. it does not depend on the particular choice of the coordinate frame.

The description of the curvature in terms of the Riemann tensor is equivalent to that in terms of sectional curvatures. According to equation (3.1) knowledge of $R^{ij}{}_{kl}$ gives the $K(S_Q)$, while the converse can also be shown: the curvatures $K(S_Q)$ for all planes S_Q at Q together with the metric tensor g_{ij} determine the Riemann tensor at the point Q (Bishop and Goldberg 1968). The relation between sectional and Gaussian curvature is a simple one. Observe that the geodesics through Q of which the tangent vectors lie in S_Q form a curved surface $\mathcal{G}(S_Q)$. K is the Gaussian curvature of this surface. When $\mathcal{G}(S_Q)$ is cap-shaped near Q the curvature K is positive; when the surface is saddle-shaped K is negative, and when the surface is locally flat $K=0$.

Now consider equation (3.1). The denominator can be written

$$x_i x^i y_j y^j - x_i y^i x_j y^j = (\delta^i{}_k\delta^j{}_l-\delta^i{}_l\delta^j{}_k)x_i x^k y_j y^l. \tag{3.2}$$

Therefore, if in a particular coordinate frame the $R^{ij}{}_{kl}$ can be written in the form

$$R^{ij}{}_{kl}=c_{ij}(\delta_{ik}\delta_{jl}-\delta_{il}\delta_{jk}), \qquad \text{(no summation convention)}$$

then c_{ij} is the sectional curvature of the plane section spanned by the tangent vectors in the q^i and q^j directions. Comparison with equation (2.27) shows that in our case

$$c_{ij}=(\lambda_i+\lambda_j-\nu_m\nu_m)/4(E-V)^3, \qquad i<j. \tag{3.3}$$

Actually the c_{ij} are the eigenvalues of a matrix constructed from the $R^{ij}{}_{kl}$. This can be shown as follows. Let $\boldsymbol{e}_i$ be the unit tangent vector in the q^i direction, and let $\boldsymbol{x}=x^i\boldsymbol{e}_i$, $\boldsymbol{y}=y^i\boldsymbol{e}_i$. Then there are $\frac{1}{2}N(N-1)$ linearly independent exterior vector products $\boldsymbol{e}_i\wedge\boldsymbol{e}_j (i<j)$. They can be denoted Ψ_α; $\alpha=1,\ldots,\frac{1}{2}N(N-1)$ representing a pair of indices $i, j (i<j)$. In the Ψ_α basis the exterior vector product $\boldsymbol{x}\wedge\boldsymbol{y}$ can be expanded according to

$$\boldsymbol{x}\wedge\boldsymbol{y}=x^i y^j \boldsymbol{e}_i\wedge\boldsymbol{e}_j=\sum_{i<j}(x^i y^j-x^j y^i)\boldsymbol{e}_i\wedge\boldsymbol{e}_j=u^\alpha\Psi_\alpha. \tag{3.4}$$

Lowering and raising of the Greek indices is effected by the matrices

$$G_{\alpha\beta} = (g_{ik}g_{jl} - g_{il}g_{jk}) \tag{3.5a}$$

and

$$G^{\alpha\beta} = (g^{ik}g^{jl} - g^{il}g^{jk}), \tag{3.5b}$$

where $\alpha = (i, j)$, $i < j$, and $\beta = (k, l)$, $k < l$. If in addition $\gamma = (m, n)$, $m < n$, then

$$G^{\alpha\beta}G_{\beta\gamma} = (\delta^i{}_m\delta^j{}_n - \delta^i{}_n\delta^j{}_m). \tag{3.6}$$

Since $i < j$ and $m < n$ this acts as the identity:

$$G^{\alpha\beta}G_{\beta\gamma}u^\gamma = u^\alpha, \tag{3.7}$$

so that one could write $G^{\alpha\beta}G_{\beta\gamma} = \delta^\alpha{}_\beta$.

The denominator of the right-hand side of equation (3.1) is seen to be equal to $u_\alpha u^\alpha$. Using $R_{ijkl} = -R_{jikl} = -R_{ijlk}$ the numerator can be written

$$\begin{aligned} R^{ij}{}_{kl}x_iy_jx^ky^l &= R_{ijkl}x^iy^jx^ky^l \\ &= \sum_{i<j}\sum_{k<l} R_{ijkl}(x^iy^j - x^jy^i)(x^ky^l - x^ly^k) \\ &= \mathcal{R}_{\alpha\beta}u^\alpha u^\beta = \mathcal{R}^\alpha{}_\beta u_\alpha u^\beta. \end{aligned} \tag{3.8}$$

This defines the matrices $\mathcal{R}_{\alpha\beta} = R_{ijkl}$ and $\mathcal{R}^\alpha{}_\beta = R^{ij}{}_{kl}$. Since $R_{ijkl} = R_{klij}$ the matrix $\mathcal{R}_{\alpha\beta}$ is symmetric, $\mathcal{R}_{\alpha\beta} = \mathcal{R}_{\beta\alpha}$. In the new notation the sectional curvature becomes

$$K = \mathcal{R}^\alpha{}_\beta u_\alpha u^\beta / u_\alpha u^\alpha. \tag{3.9}$$

If $\boldsymbol{u}$ is an eigenvector of $\mathcal{R}^\alpha{}_\beta$ with eigenvalue λ_u, i.e. $\mathcal{R}^\alpha{}_\beta u^\beta = \lambda_u u^\alpha$, then $K = \lambda_u$ for the plane section defined by $\boldsymbol{u}$. Clearly the eigenvalues of $\mathcal{R}^\alpha{}_\beta$ are invariants. In order to find them we use the fact that there exists a real coordinate transformation which transforms g_{ij} into the unit matrix. The new coordinate system is called orthonormal. In the orthonormal frame it is not necessary to distinguish between upper and lower indices. In particular $R^{ij}{}_{kl} = R_{ijkl}$, which means that $\mathcal{R}^\alpha{}_\beta$ is a symmetric matrix. One easily sees that in the orthonormal frame $R^{ij}{}_{kl}$ is given by equation (2.27), and that this expression corresponds to the diagonal form of $\mathcal{R}^\alpha{}_\beta$. Comparison with equation (3.9) then shows that the eigenvalues of $\mathcal{R}^\alpha{}_\beta$ are just the curvatures c_{ij} defined by equation (3.3). For this reason the curvatures $c_{ij}(i < j)$ will henceforth be called eigencurvatures.

3.2. Elementary properties of the eigencurvatures

Suppose that the potential is a sum of pair interactions and that $Q^i (i = 1, 2, 3)$ are the centre-of-mass coordinates. Then $\partial V/\partial Q^i = 0$ and $\partial^2 V/\partial Q^i \partial Q^j = 0$ $(i, j = 1, 2, 3)$. This shows that μ_{ij} has at least three eigenvalues equal to zero. With equation (3.3) this implies that at least three eigencurvatures are negative.

More generally, let μ_{ij} have N_0 eigenvalues equal to zero, the other eigenvalues being different from zero. Let the eigenvalues be ordered in such a way that $\lambda_1 = \lambda_2 = \ldots = \lambda_{N_0} = 0$. Then $\frac{1}{2}N_0(N_0 - 1)$ eigencurvatures have the value

$$-\nu_m\nu_m/4T^3. \tag{3.10}$$

Here and in the remainder of this section T denotes the kinetic energy:

$$T = E - V(q). \tag{3.11}$$

Assuming $\lambda_{N_0+i} \neq \lambda_{N_0+j}$ for $i \neq j$, the eigencurvature

$$(\lambda_{N_0+i} - \nu_m \nu_m)/4T^3 \qquad i = 1, \ldots, N - N_0 \tag{3.12}$$

is N_0-fold degenerate. There are $N_0(N-N_0)$ eigencurvatures of this type. The eigencurvature

$$(\lambda_{N_0+i} + \lambda_{N_0+j} - \nu_m \nu_m)/4T^3 \qquad i, j = 1, \ldots, N - N_0 \tag{3.13}$$

at last is nondegenerate (still assuming $\lambda_{N_0+i} \neq \lambda_{N_0+j}$). There are $\binom{N-N_0}{2} = \frac{1}{2}(N-N_0)(N-N_0-1)$ eigencurvatures of this type.

Next consider the asymptotic behaviour of the c_{ij} as given by equation (3.3) for large energies, $E \to \infty$. Let the eigenvalues of ν_{ij} be denoted $\lambda_i^{(0)}$. Then it follows from equations (2.25) and (3.3) that

$$c_{ij} = (\lambda_i^{(0)} + \lambda_j^{(0)})/2T^2 + O(1/T^3). \tag{3.14}$$

Using equation (2.29) one finds

$$R = 2 \sum_{\substack{i,j \\ i<j}} c_{ij} = \frac{N-1}{T^2} \operatorname{Tr}(\nu_{ij}) + O\left(\frac{1}{T^3}\right) \tag{3.15}$$

for the asymptotic behaviour of the Riemann scalar.

From equations (3.14) and (3.15) one concludes that for large energies the curvature is essentially determined by the matrix ν_{ij} of the second derivatives of the potential.

Another limiting case is represented by the boundary of the physical region. The boundary is defined by $T = 0$. As one approaches the boundary $T \to 0$ and equation (2.25) shows that

$$\mu_{ij} \to 3\nu_i \nu_j \qquad \nu_m \nu_m \neq 0,\ T \to 0. \tag{3.16}$$

This limiting matrix has one eigenvalue $3\nu_m \nu_m$ while all other eigenvalues vanish. Consequently the limiting behaviour of $N-1$ eigencurvatures is given by

$$c_{ij} = \nu_m \nu_m / 2T^3 + O(1/T^2), \tag{3.17a}$$

while for the other $\frac{1}{2}(N-1)(N-2)$ eigencurvatures one has

$$c_{ij} = -\nu_m \nu_m / 4T^3 + O(1/T^2). \tag{3.17b}$$

Calculation of twice the sum of the eigencurvatures gives the Riemann scalar:

$$R = -\frac{(N-1)(N-6)}{4T^3} \nu_m \nu_m + O\left(\frac{1}{T^2}\right). \tag{3.18}$$

These expressions show that, sufficiently close to the boundary of the physical region (i.e. T sufficiently small), the Riemann scalar always becomes negative. Also we find that the curvature in a neighbourhood of the boundary is determined by the first derivatives of the potential, i.e. by the forces. This should be compared with the behaviour for $E \to \infty$, in which case the curvature expressions only contained the second derivatives of V.

To conclude this section, consider a system for which an equilibrium configuration is accessible. In an equilibrium configuration $\nu_i = \partial V / \partial q^i = 0 (i = 1, \ldots, N)$, hence $\mu_{ij} = 2(E-V)\nu_{ij}$. Let the eigenvalues $\lambda_i^{(0)}$ of $\nu_{ij} = \partial^2 V / \partial q^i \partial q^j (i, j = 1, \ldots, N)$ be strictly

positive, so that by Liapunov's theorem (Hirsch and Smale 1974) the equilibrium is stable. Then

$$c_{ij} = (\lambda_i^{(0)} + \lambda_j^{(0)})/2T^2 > 0, \qquad i, j = 1, \ldots, N, \tag{3.19}$$

showing that all eigencurvatures, and therefore also the Riemann scalar, are positive in a neighbourhood of the equilibrium configuration.

4. Manifolds of negative curvature

A manifold is said to have negative curvature if all sectional curvatures are negative everywhere (Helgason 1962). Definition (3.1) shows that this is equivalent to the condition that everywhere on the manifold

$$R_{ijkl}x^i y^j x^k y^l < 0 \quad \text{for all tangent vectors } \boldsymbol{x}, \boldsymbol{y}. \tag{4.1}$$

The implications of this inequality for the geometry of the geodesics can be inferred from the equation of geodesic deviation. Consider a differentiable family of geodesics $q(t, s)$ parametrised by a scalar t, each geodesic in the family being parametrised by the arc-length parameter s. Then the geodesic deviation $\boldsymbol{w}$ is defined as $\partial/\partial t$, or in more pictorial language, as the limit $\partial q/\partial t$ of the separation $\Delta q/\Delta t$ per unit of t between points on neighbouring geodesics with equal s. Let $\dot{\boldsymbol{q}} = \partial q/\partial s$ be the unit tangent vector to some geodesic in the family and $\boldsymbol{w}$ the geodesic deviation, and let D denote the covariant derivative along the geodesic. Then the equation of geodesic deviation (Adler *et al* 1965) can be written

$$D^2 w^i/\mathrm{d}s^2 = -R^i{}_{jkl}\dot{q}^j w^k \dot{q}^l. \tag{4.2}$$

Now

$$\frac{D^2}{\mathrm{d}s^2}(w_i w^i) = 2\frac{Dw_i}{\mathrm{d}s}\frac{Dw^i}{\mathrm{d}s} + 2w_i\frac{D^2 w^i}{\mathrm{d}s^2}, \tag{4.3}$$

which upon substitution of equation (4.2) becomes

$$\frac{D^2}{\mathrm{d}s^2}(w_i w^i) = 2\frac{Dw_i}{\mathrm{d}s}\frac{Dw^i}{\mathrm{d}s} - 2R_{ijkl}w^i\dot{q}^j w^k \dot{q}^l. \tag{4.4}$$

If (4.1) holds it follows that

$$\frac{D^2}{\mathrm{d}s^2}(\boldsymbol{w} \cdot \boldsymbol{w}) > 0. \tag{4.5}$$

Therefore geodesics on a surface $\mathcal{G}(S_Q)$ which is negatively curved near Q, i.e. $K(S_Q) < 0$, will be diverging near Q. For a manifold of negative curvature the inequality (4.5) suggests that the distance between neighbouring geodesics is a convex function of the arc length, that is, a function curving away from the s axis.

The argument using the geodesic deviation holds only in an infinitesimal neighbourhood of a point. It can however be extended to yield a theorem on the local behaviour of the geodesics. To formulate this theorem, let $q(s)$ and $q'(s')$ be two geodesics, and $s' = as + b$ with a and b real numbers. Furthermore, let the length L of a curve $q(\lambda)$, $0 \leqslant \lambda \leqslant 1$, between the points $Q_1 = q(0)$ and $Q_2 = q(1)$ be defined by

$L(q) = \int_0^1 (\dot{\boldsymbol{q}} \cdot \dot{\boldsymbol{q}})^{1/2} \, d\lambda$, and the distance ρ between Q_1 and Q_2 as

$$\rho(Q_1, Q_2) = \inf_{\substack{q(\lambda) \\ q(0)=Q_1, q(1)=Q_2}} L(q). \tag{4.6}$$

Suppose that there is only one geodesic connecting the points $q(s)$ and $q'(s')$ for $\sigma < s < \Sigma$. Then for $\sigma < s < \Sigma$ the distance between $q(s)$ and $q'(s')$ is a convex function of s. For proofs of this and other theorems on the divergence of geodesics on manifolds of negative curvature the reader is referred to Busemann (1955). When some of the sectional curvatures are positive, the first term on the right-hand side of equation (4.4) shows that in general it will not be possible to draw a conclusion about the convergence or divergence of the geodesics.

Let us now consider a property of a manifold of negative curvature which is of great interest for the ergodic theory of statistical mechanics, namely the Lobatchevsky–Hadamard theorem (Arnol'd and Avez 1968). This theorem states that the geodesic flow on a closed Riemannian manifold of negative curvature is a C-flow. Heuristically a C-flow is a flow in which all trajectories diverge exponentially with respect to both past and future. A formal definition of a C-flow can be found in Arnol'd and Avez (1968). Next we note that if a geodesic flow is a C-flow, then according to Anosov (1967) it is a K-system. So, for a conservative system in classical mechanics, the Lobatchevsky–Hadamard theorem and Anosov's result imply that if the manifold $E - V \geqslant 0$ is closed and if all eigencurvatures c_{ij} are negative, then the system is a K-system.

For a definition of a K-system the reader is once more referred to Arnol'd and Avez (1968). Here we recall that the most easily visualised property of a K-system is that it is mixing of all degrees. This means the following. Let P be a point in the phase space Γ, $P = p, q \in \Gamma$. Then the translation T_t over a time interval t is defined by $T_t P = p(t), q(t)$. Consider some measurable set $A \subset \Gamma$. The measure of A is denoted $\mu(A)$. Assume $\mu(\Gamma) < \infty$ so that μ can be normalised: $\mu(\Gamma) = 1$. Then the system is mixing of degree n if for any n-tuple of measurable sets $A_1, \ldots, A_n \subset \Gamma$

$$\lim_{\min_{i \neq j} |t_i - t_j| \to \infty} \mu(T_{t_1} A_1 \cap \ldots \cap T_{t_n} A_n) = \mu(A_1) \ldots \mu(A_n). \tag{4.7}$$

The case $n = 2$ corresponds to what is simply called mixing. In its turn, mixing implies ergodicity.

One sees that a K-system is quite high in the hierarchy of ergodicity, and that consequently the geodesic flow on a manifold of negative curvature must be very erratic.

In principle the Lobatchevsky–Hadamard theorem enables one to establish whether a classical mechanical system with a given potential is a K-system. All one has to do is compute the eigencurvatures (3.3) and check whether they are negative everywhere. Regrettably equation (3.17) shows that near the border of the physical region there are always positive eigencurvatures (even though for $N \geqslant 7$ the averages of the eigencurvatures and the Riemann scalar are negative). Therefore the curvature calculations can at most prove local C-system behaviour of the system. They cannot be used to prove (or disprove) that the system is a K-system, which is a global property.

5. Two simple examples: the Kepler and Hénon–Heiles problems

Both problems have two degrees of freedom, so that the Riemann tensor is a scalar and $R = 2R^{12}{}_{12}$. It therefore suffices to compute R according to equation (2.30).

Let us first consider the Kepler or gravitational two-body problem. We take $V(x, y) = -1/r = -(x^2+y^2)^{-1/2}$ and assume $\alpha_{ij} = \delta_{ij}$. Substitution of the derivatives of V in equation (2.30) yields

$$R = -\frac{E}{(E-V)^3}\frac{1}{r^3}. \tag{5.1}$$

This shows that the curvature is positive when $E<0$, i.e. for elliptic orbits. A small variation of initial conditions at constant E will change such an orbit only a little. Indeed, elliptic orbits are stable in the sense of Liapunov. The distance between points on neighbouring elliptic orbits is a periodic function of time.

For parabolic orbits $R = E = 0$.

For hyperbolic orbits $E>0$ and the curvature is negative. One easily verifies that the distance between points on different hyperbolae is a convex function of time. Since the configuration space is unbounded, the negative curvature does not imply that the system is a C-system.

The configuration space of the Hénon–Heiles (1964) potential

$$V(x, y) = \tfrac{1}{2}(x^2+y^2+2x^2y-\tfrac{2}{3}y^3) \tag{5.2}$$

is bounded for $E<\frac{1}{6}$. But for this system one finds

$$R = \frac{1}{(E-V)^2}\left[2+\frac{1}{E-V}\left\{\left(\frac{\partial V}{\partial x}\right)^2+\left(\frac{\partial V}{\partial y}\right)^2\right\}\right]>0. \tag{5.3}$$

This result may be compared with the local stability analysis of Toda (1974, see also Brumer and Duff 1976). These authors define local instability and divergence of trajectories in terms of the matrix $\nu_{ij} = \partial^2 V/\partial q^i \partial q^j$: the system shows local instability and the trajectories are said to diverge if one of the eigenvalues of ν_{ij} is negative. Since ν_{ij} is not a tensor, such a definition depends on the coordinatisation, as pointed out already by Benettin *et al* (1977). If one wants to define (local) stability and instability properties in a coordinate-independent way this should be done in terms of suitable tensors.

In the Hénon–Heiles system Toda finds local divergence of trajectories for $(x^2+y^2)^{1/2}>\frac{1}{2}$, that is, for $E>\frac{1}{12}$ the system shows exponential instability in part of phase space. However, this does not allow one to conclude that the system is a C-system. Our result (5.3) on the other hand does not exclude the possibility that one can find a coordinate frame in which ν_{ij} has negative eigenvalues.

6. The calculation of the curvature statistics

The curvature statistics have been calculated as a function of the number density n and the total energy E. The number density determines the size of the cube containing the particles. The sides of the cube have length L such that $N_p/L^3 = n$, $N_p = 8, 16$ being the number of particles.

The MNF (Minnesota Fortran) random-number generator is used to generate random positions for the particles. For those configurations which have a positive kinetic energy, $(E-V)>0$, the curvature is calculated. In other words, we are sampling the part of configuration space where $(E-V)>0$.

The curvature is calculated by diagonalising the matrix μ_{ij}. The algebra of the computation is straightforward. The eigenvalues are computed by Jacobi's method as adapted from Carnahan *et al* (1969), and the errors were checked using Gershgorin's inequalities (Fröberg 1969). Using equation (3.3) the eigenvalues of μ_{ij} yield the eigencurvatures. According to § 3 the total number of eigencurvatures is $\frac{1}{2}N(N-1)$. Here $N = 3N_p$, so an 8-particle system has 276 and a 16-particle system 1128 eigencurvatures. The number of negative eigencurvatures of a configuration will be designated N_-. Using the first equality of equation (3.15) one obtains the Riemann curvature scalar.

Having calculated these quantities for an ensemble of randomly chosen configurations, one can derive the distributions of the eigencurvatures c_{ij}, the number of negative eigencurvatures N_- and of the Riemann scalar R. They are denoted P_c, P_- and P_R, respectively. The distributions will be presented as histograms. P_c is normalised to 276 and 1128 for the 8- and 16-particle systems respectively, while P_- and P_R are normalised to 1. The number of configurations in an ensemble has been chosen such that a relative standard error of the order of 10% in the larger values of the distributions was obtained. The errors are indicated in the graphs. For some small values no error bar has been drawn in the graphs. In these cases the absolute error is negligible. It has been verified that the numerical errors in the eigenvalues do not affect the distribution functions.

The graphs also give the ensemble average $\bar{V}$ of the potential energy and the ensemble average $\bar{N}_-$ of the number of negative eigencurvatures. The errors given for these quantities are the standard errors in the mean.

It turns out that, in general, the eigencurvatures of a given configuration and those of different configurations are of very different orders of magnitude. For this reason a logarithmic scale is used in the graphs of P_c and P_R.

7. Curvature statistics for Debye–Hückel systems

The Debye–Hückel potential is given by $V(r) = e^{-\kappa r}/r$, κ^{-1} being the range of the potential. It provides a model for hot dilute plasmas (see e.g. Chen 1974) and for dilute solutions of electrolytes (see e.g. Münster 1974). It is convenient to choose the unit of length equal to κ^{-1}. The potential of the N_p-particle system can then be written as

$$V(\boldsymbol{r}_1, \ldots, \boldsymbol{r}_{N_p}) = \sum_{\substack{i,j=1 \\ i<j}}^{N_p} \frac{\exp(-r_{ij})}{r_{ij}}, \qquad r_{ij} = |\boldsymbol{r}_i - \boldsymbol{r}_j|. \tag{7.1}$$

Curvature calculations have been made for the densities $n = 0{\cdot}001$, $n = 1$ and $n = 1000$. These densities correspond to average interparticle distances of the order of 10, 1 and $0{\cdot}1$ respectively. For each of the densities, at least three energies have been considered. For low energies the first term in the right-hand side of equation (2.25) dominates, for intermediate energies both terms are of the same order of magnitude, while for high energies the second term dominates. That is, for low energies the curvature is mainly determined by ∇V, and at high energies by the second derivatives $\partial^2 V/\partial q^i \partial q^j$. The results of the computations for the 8-particle system are given in figure 1 for $n = 0{\cdot}001$, figure 3 for $n = 1$ and figure 5 for $n = 1000$. Those for 16 particles are given in figures 2, 4 and 6 for $n = 0{\cdot}001$, $n = 1$ and $n = 1000$ respectively.

8 particles. First let us consider the eigencurvature distributions P_c. At all densities and for every energy one notices a group of negative and a smaller group of positive eigencurvatures. At low energies the first group is several times larger than the second. The fraction of negative eigencurvatures steadily decreases with increasing energy, but even at the highest energies considered here it still exceeds the fraction of positive eigencurvatures.

Because of the denominator in equation (3.3) the absolute values of the eigencurvatures decrease with increasing energy. Therefore the two groups will move in the direction of zero as E increases. One further observes that the peaks tend to sharpen with increasing density, or to put it the other way around, they tend to broaden with decreasing density. The explanation for this is to be found in the range of configurations accessible to the system, which is greater at lower densities. Given that the particles are confined to a box, they can still be close at low density, but at high density they cannot be far apart.

The distributions P_- of the number of negative eigencurvatures show that for nearly all configurations the majority of the eigencurvatures is negative. However, none of the configurations has only negative eigencurvatures, or 254 or more negative eigencurvatures for that matter. In the low-energy cases, the high peak in the last interval but one is caused by the large fraction of configurations with $N_- = 253$. These configurations represent the limiting case (3.17) or $(E - V) \to 0$. The percentages for the lowest energies are given in the following table:

$n = 0{\cdot}001$	$E = 0{\cdot}01$	$36 \pm 3\%$
$n = 1$	$E = 10$	$37 \pm 3\%$
$n = 1000$	$E = 250$	$32 \pm 3\%$.

For all densities the average number of negative eigencurvatures $\bar{N}_-$ decreases with increasing energy.

Though the eigencurvature distributions at corresponding energies are rather similar, the Riemann scalar distributions P_R turn out to be very different.

At low densities a large part of the Riemann scalars is positive even for low energies. The fraction of negative curvature scalars decreases with increasing energy and would seem to vanish for very high energy.

The density $n = 1$ is found to represent an intermediate case: at low energies all Riemann scalars are negative, at high energies they are nearly all positive. The transition between the case of negative and the case of positive Riemann scalars is not a sharp one, but at $E = 50$ about half of the Riemann scalars is negative, half positive.

At high densities and not too high energies the Riemann scalar is negative everywhere. Only at very high energy does one find an appreciable fraction of positive Riemann scalars.

In addition to the distributions P_c, P_- and P_R and the averages $\bar{V}$ and $\bar{N}_-$ we could also have given the average of R for each (n, E) pair considered. This average is found to be rather meaningless, however. It is determined entirely by the extremal values in the R distribution. It could not therefore be evaluated reliably in the present study.

With respect to the number of random configurations needed in order to obtain sufficiently small standard errors in the distributions, one observes that more configurations are needed at the lower energies. This is apparently due to the shape of $V(\boldsymbol{r}_1, \ldots, \boldsymbol{r}_N)$ considered as a $3N$-dimensional surface. At low energies $(E - V)$ turns

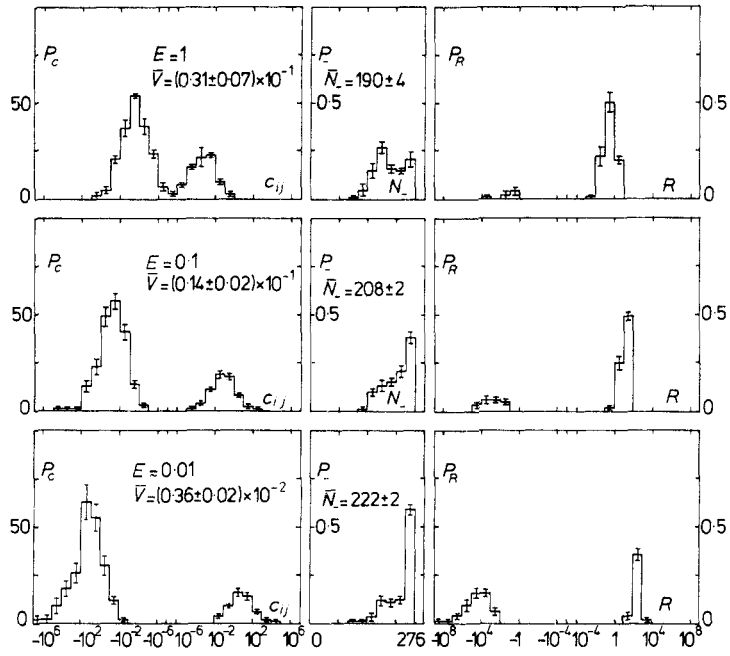

Figure 1. Curvature statistics of an 8-particle DH system for $n = 0{\cdot}001$. The number of configurations in the samples is 200 for $E = 0{\cdot}01$ and $E = 0{\cdot}1$, and 100 for $E = 1$.

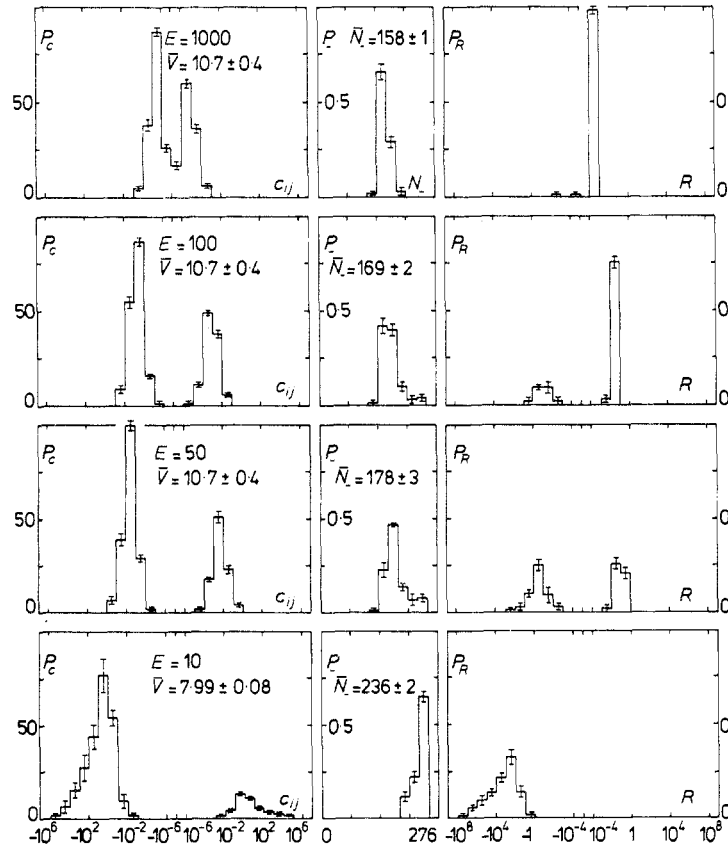

Figure 3. Curvature statistics of an 8-particle DH system for $n = 1$. The number of configurations in the sample for $E = 10$ is 200; for the other energies it is 100.

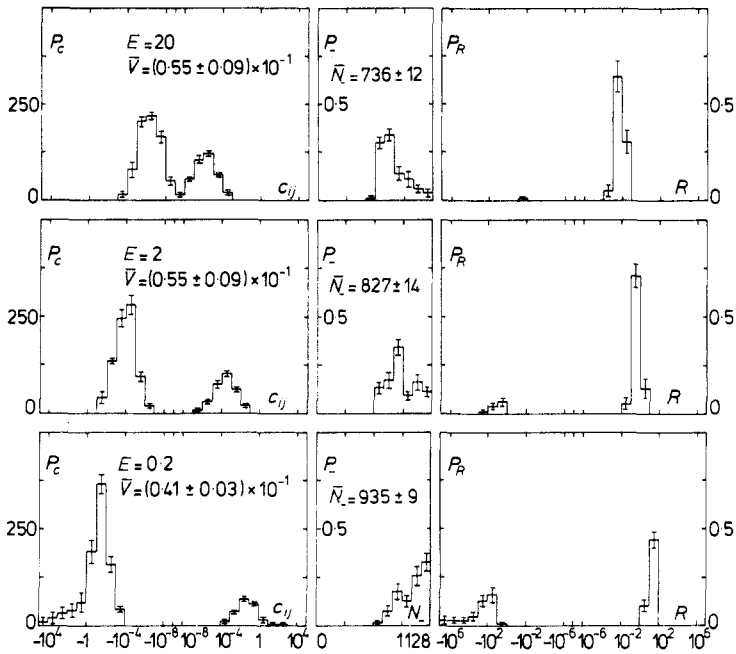

Figure 2. Curvature statistics of a 16-particle DH system for $n = 0{\cdot}001$. At each of the energies the number of configurations in the sample is 100.

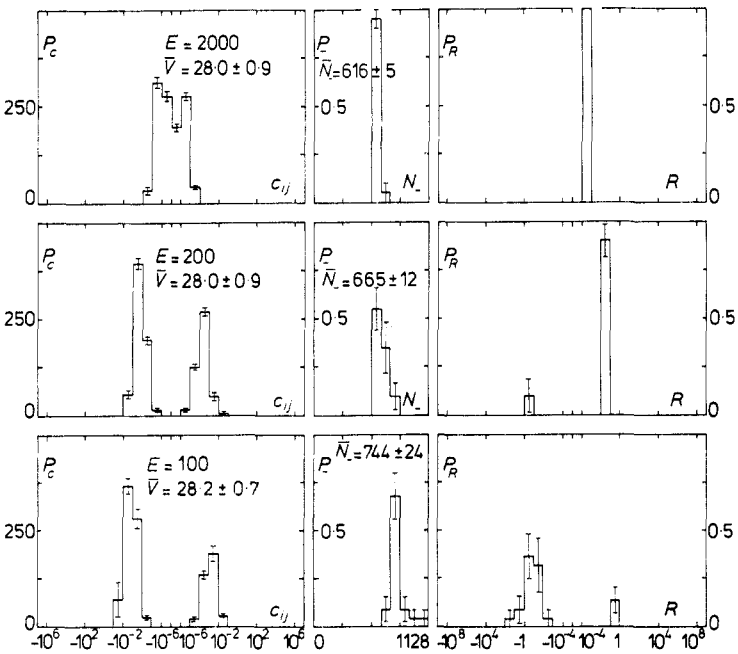

Figure 4. Curvature statistics of a 16-particle DH system for $n = 1$. The number of configurations in the sample for $E = 100$ is 22; for the other energies it is 20.

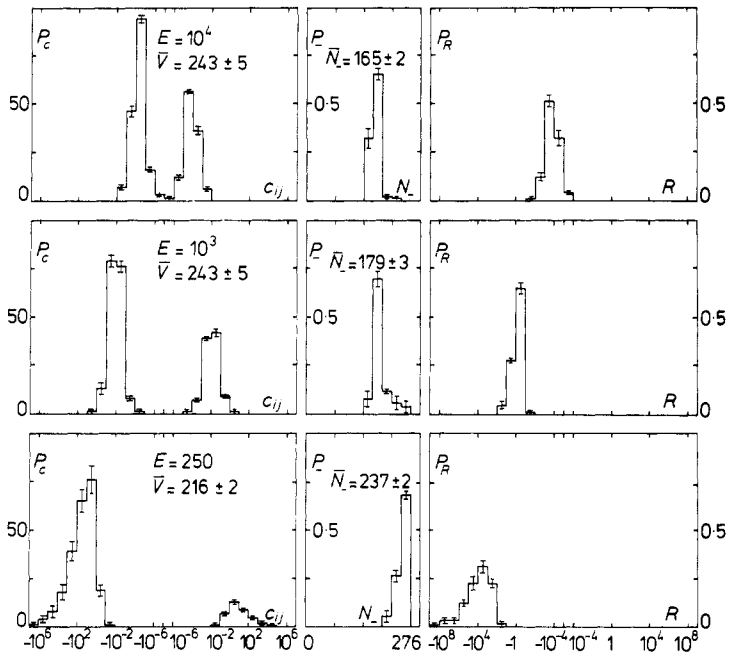

Figure 5. Curvature statistics of an 8-particle DH system for $n = 1000$. The number of configurations in the samples is 200 for $E = 250$ and 100 for the higher energies.

out to vary relatively strongly over the accessible part of configuration space. Since $(E - V)$ enters the curvature formulae through both (2.25) and (3.3), this results in a larger spread in the number of eigencurvatures in a given interval.

16 particles. The curvature distributions for the 16-particle Debye–Hückel systems are given in figures 2, 4 and 6. The distributions for $n = 1$, $E = 20$ are not given there since the eigencurvatures are of too many different orders of magnitude, making it impossible to obtain acceptable statistics in the computer time available. However, the case of 1081 negative and 47 positive eigencurvatures (corresponding to $N_- = 253$ for the 8-particle system) was found for $70 \pm 8\%$ of the configurations sampled. At $E = 100$ this fraction has decreased to $\leqslant 5\%$. The last estimate also holds for $n = 1000$, $E = 1000$. For $n = 0{\cdot}001$, $E = 0{\cdot}2$ the limiting behaviour was found for $14 \pm 4\%$ of the configurations. These fractions are appreciably lower than the corresponding ones for 8 particles; in other words, the fractional volume of the boundary region of the domain $E - V > 0$ is much smaller. But this is to be expected since the fractional volume of the boundary region of $E - V > 0$ in the 48-dimensional configuration space of the 16-particle system will in general be much less than the corresponding fraction in the 24-dimensional configuration space of the 8-particle system.

Comparison of figures 1 and 2 for $n = 0{\cdot}001$, 3 and 4 for $n = 1$ and 5 and 6 for $n = 1000$ shows that at a given density the behaviour of the curvature of the 8- and 16-particle systems is strikingly similar. The similarity is perhaps most clearly demonstrated in the R-distribution histograms. There one finds that for $n = 0{\cdot}001$ most R values are positive, while for $n = 1000$ nearly all R-values are negative, irrespective of

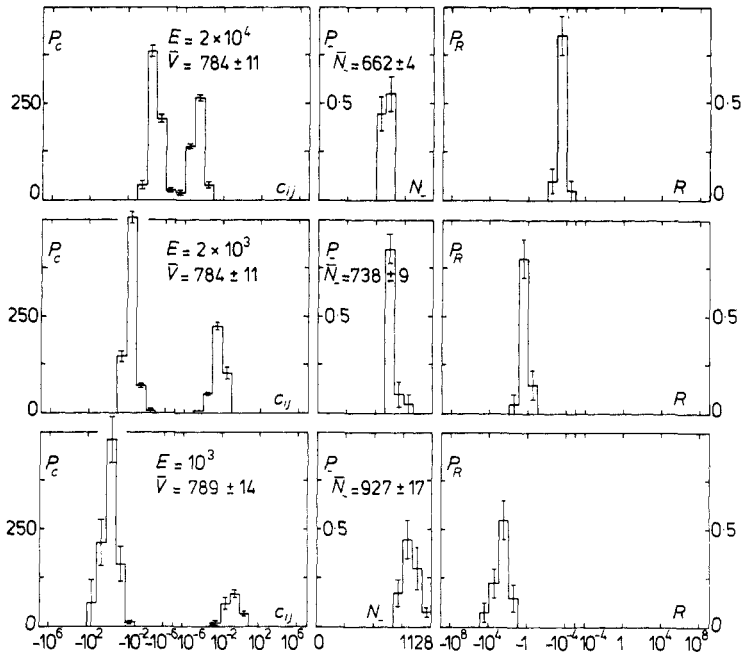

Figure 6. Curvature statistics of a 16-particle DH system for $n = 1000$. The number of configurations in the samples is 40 for $E = 1000$ and 20 for the higher energies.

the number of particles in the system. At $n = 1$ and low energies most R-values are negative, but at high energies nearly all are positive.

One concludes that the qualitative properties of the curvature distribution functions which we have calculated here are meaningful not only for one particular number of particles, but are characteristic at least for systems with O(10) particles. The quantitative differences, which are most pronounced at $n = 0{\cdot}001$, have to be explained by the factor $(E - V)$ in equations (2.25) and (3.3), and as boundary effects.

A remark should be made here with respect to the distributions P_- of the number of negative eigencurvatures. Several of the histograms of these distributions for the 8-particle system show a gap in the last interval, which represents $254 \leqslant N_- \leqslant 276$. Clearly this gap is somewhat artificial: the important case of $N_- = 253$ is included in the last interval but one. The corresponding case for the 16-particle system, $N_- = 1081$, is included in the last interval, which extends from 1034 to 1128.

8. Curvature statistics for Lennard–Jones systems

As a representative example of a potential with a short-range repulsive and a long-range attractive part let us consider the Lennard–Jones potential

$$V(r) = 4\epsilon\{(\sigma/r)^{12} - (\sigma/r)^6\}. \tag{8.1}$$

This is a realistic model for the interaction between the atoms of noble gases such as Ar (see Barker and Henderson (1976) for equilibrium, and Copley and Lovesey (1975) for

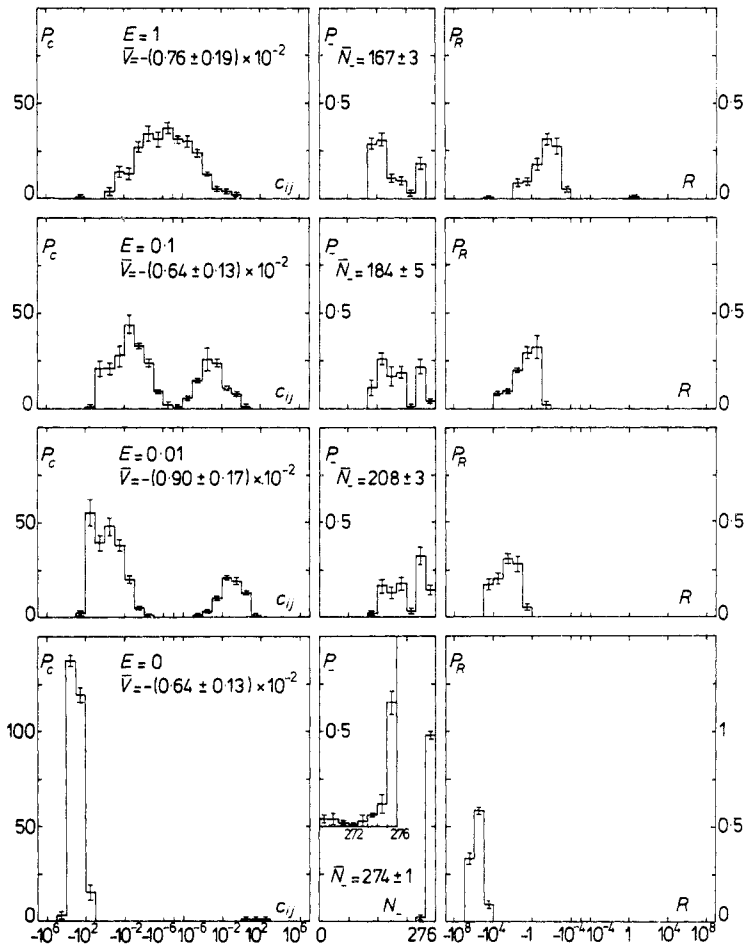

Figure 7. Curvature statistics of an 8-particle LJ system for $n = 0{\cdot}001$. The number of configurations in the samples is 100 for $E = 0$ and $E = 0{\cdot}1$, and 200 for $E = 0{\cdot}01$ and $E = 1$.

dynamical properties). It is convenient to choose σ as the unit of length, and units of mass and time such that $4\epsilon = 1$. Then the potential of an N_p particle LJ system is given by

$$V(\boldsymbol{r}_1, \ldots, \boldsymbol{r}_{N_p}) = \sum_{\substack{i,j=1 \\ i<j}}^{N_p} \left(\frac{1}{r_{ij}^{12}} - \frac{1}{r_{ij}^{6}} \right), \qquad r_{ij} = |\boldsymbol{r}_i - \boldsymbol{r}_j|. \tag{8.2}$$

For Ar, using Raman's value of ϵ as quoted by Copley and Lovesey (1975), the kinetic energy $\frac{3}{2}$ kT per particle at 90K is about 0·3 and at 273K about 1.

8 particles. For the LJ potential we have studied the densities $n = 0{\cdot}001$ and $n = 1/\sqrt{2} \simeq 0{\cdot}707$, which correspond to the gas and liquid phase of Ar respectively, if we use Raman's value of σ and the experimental data given in Gray (1957). The lowest energy considered in both cases is $E = 0$. For $n = 0{\cdot}001$ at this energy, the two terms in equation (2.25) in general are of the same order of magnitude. For $n = 1/\sqrt{2}$, however,

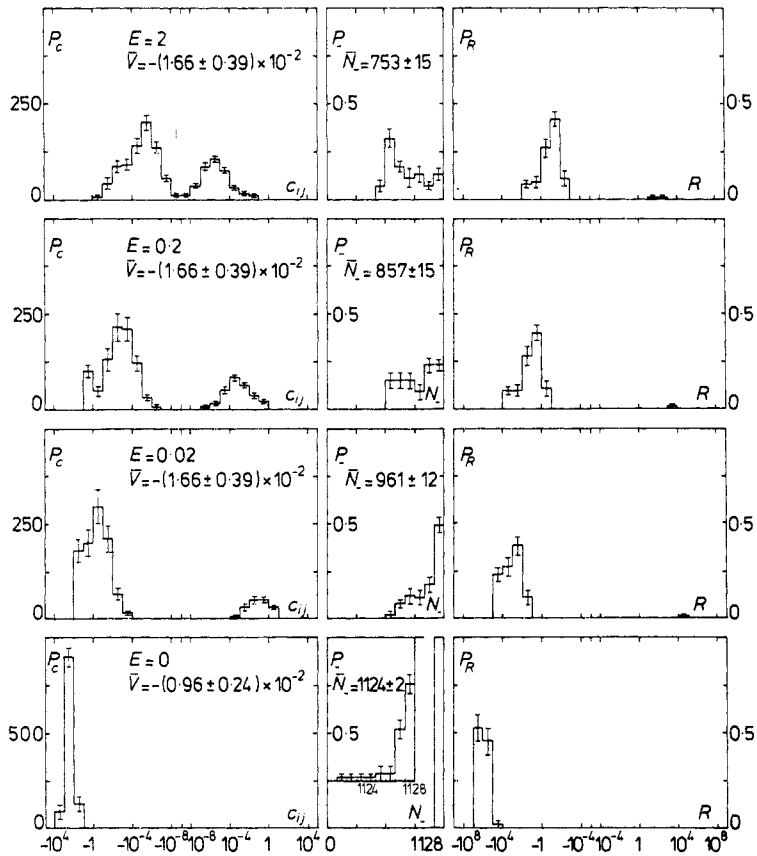

Figure 8. Curvature statistics of a 16-particle LJ system for $n = 0{\cdot}001$. The number of configurations in the sample for $E = 0$ is 51; for the other energies it is 100.

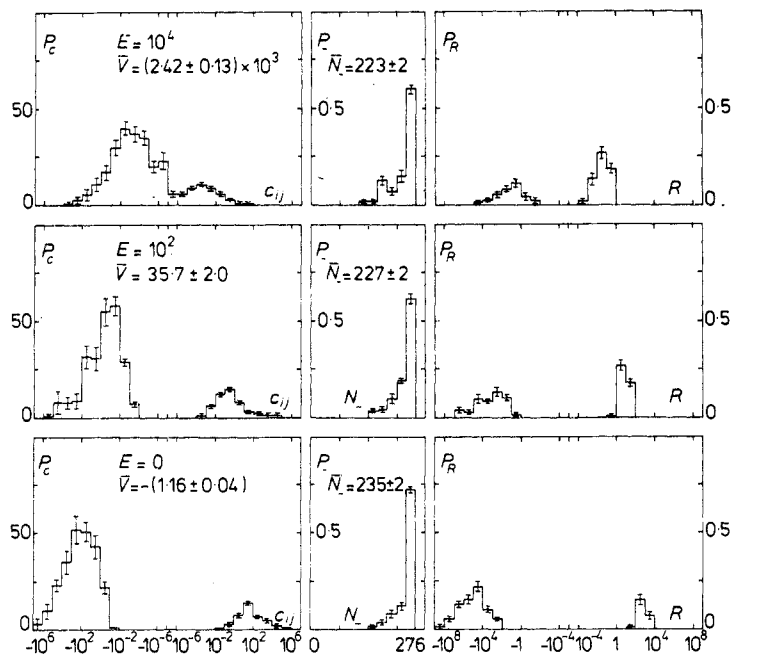

Figure 9. Curvature statistics of an 8-particle LJ system for $n = 1/\sqrt{2}$. At each of the energies the number of configurations in the sample is 200.

the $\nu_i\nu_j$ term is often much larger than the ν_{ij} term. In fact at $E = 0$ the combination of 253 negative and 23 positive eigencurvatures is found for $50 \pm 4\%$ of the configurations. For $n = 0{\cdot}001$ only two of the 100 configurations sampled had $N_- = 253$.

For $n = 0{\cdot}001$ the highest energy considered is $E = 1$. Here it is found that, on average, the term $(E - V)\nu_{ij}$ is much larger than $\nu_i\nu_j$, and that the curvature is essentially determined by ν_{ij}. For $n = 1/\sqrt{2}$ the highest energy considered is $E = 10^4$. This is not a high energy in the sense of equation (3.14): the curvature is not found to be dominated by ν_{ij}.

The eigencurvature distributions P_c (figures 7–9) show a superficial resemblance to those of the DH systems. There are two groups of eigencurvatures, namely a group of negative eigencurvatures and a group of positive ones. At low energies, the total number of negative eigencurvatures in the ensemble is several times the number of positive eigencurvatures, but with increasing E the fractions tend to become equal. Also with increasing E the absolute values of the eigencurvatures decrease in accordance with equation (3.3).

Let us now take a closer look at the case of $n = 0{\cdot}001$ (see figure 7). The curvature at $E = 0$ is extremely interesting in that for $65 \pm 6\%$ of the configurations all eigencurvatures are negative. The detailed distribution of the number of negative eigencurvatures is shown in the inset of figure 7. (Three values fall outside the range of this figure: one case of 265 and two cases of 253 negative eigencurvatures.) Perhaps it should be remarked that the case of negative curvature ($N_- = 276$) is quite different from the limiting case of 253 negative eigencurvatures as defined by equation (3.17). The last situation is caused by the peculiar form of μ_{ij} in the limit $(E - V) \to 0$, which results in only one non-zero eigenvalue. Equations (3.17*a*, *b*) show that the resulting positive eigencurvatures are of the same order of magnitude as the negative ones. In this sense one cannot say this limiting case is close to (completely) negative curvature.

At $E = 0{\cdot}01$ negative curvature is found for only $6 \pm 2\%$ of the configurations. The eigencurvature distribution and the distribution of the number of negative eigencurvatures have changed drastically. As E increases still further to $0{\cdot}1$ and 1 the distributions change more gradually. The distribution P_- of the number of negative eigencurvatures is found not to be very smooth. In particular, the dip in this distribution for $208 \leqslant N_- \leqslant 230$ seems to be statistically significant. Since the energies $E = 0{\cdot}1$ and $E = 1$ represent the high-energy case this could be due to a peculiarity of the eigenvalue distribution of ν_{ij}.

The Riemann scalar was found to be negative for all configurations and energies considered at this density, with a single exception: one positive curvature scalar out of 200 was found at $E = 1$.

For the liquid density quite different statistics are found (see figure 9). The eigencurvature distributions are of the type met in the low-density DH systems (cf figures 1 and 2). At $E = 10^4$ the number of negative eigencurvatures is still much larger than the number of positive eigencurvatures. No negative curvature configuration was found at this density. Indeed, there was no configuration with $N_- \geqslant 254$. The distribution of the number of negative eigencurvatures resembles a flight of stairs for all E, excepting the deviation at $E = 10^4$ which could be of a statistical nature. At all energies considered the fraction of configurations with $N_- = 253$ is rather large. The percentages are:

E	0	10	10^2	10^3	10^4
$p_{N_-=253}$	50 ± 4	44 ± 3	38 ± 2	39 ± 2	38 ± 3.

This large and consistent fraction should probably be explained as a consequence of the high density. The high density means close pairs, which together with the strong r-dependence of the LJ potential (equation 8.1) result in dominance of the $\nu_i\nu_j$ term in equation (2.25).

The Riemann scalar distributions show not only that there is no case of negative curvature but also that there is not an energy at which all Riemann scalars are negative. At $E=0$ the percentage of positive curvature scalars is 24 ± 3, and this percentage increases monotonically to 62 ± 3 at $E=10^4$. Note that this trend is hardly discernible (if at all) in the histograms for P_c.

16 particles. The curvature distributions of the 16-particle LJ system have been determined only for $n=0{\cdot}001$. For $n=1/\sqrt{2}$ it was not possible to construct a sufficiently large ensemble in the time available. We note that $8=2^3$ particles at liquid density easily fit into a cube, but for 16 particles the fitting problem is forbidding.

For $n=0{\cdot}001$ figure 8 shows good agreement with figure 7 of the results for 8 particles. At $E=0$ the percentage of configurations with negative curvature is $51\pm5\%$. This is a bit less than the $65\pm6\%$ in the 8-particle case, but on the other hand the percentage of negative curvatures has increased from $99{\cdot}5\pm0{\cdot}1$ to $99{\cdot}7\pm0{\cdot}2$ per cent.

9. Concluding remarks

In § 3 it was shown that a conservative system cannot have negative curvature sufficiently close to the boundary of the physical region. In the two preceding sections it was found that negative curvature is also a rare phenomenon farther away from the boundary. Negative curvature seems to be too strong a condition for conservative systems, implying a degree of complexity of the trajectories encountered at most locally. As a topic for further research it would be interesting to delimit the regions of negative curvature and to compare their size with that of the eigencurvatures.

A much weaker condition which a conservative system theoretically could satisfy is that the Riemann curvature scalar is negative everywhere. This is equivalent to the condition that the average of the eigencurvatures is negative everywhere. In several of the DH and LJ systems considered above no configuration was encountered with a positive Riemann scalar. Perhaps it is possible to give a formal proof of $R<0$ everywhere for certain potentials in appropriate ranges of density and energy. But now there is another difficulty in that it does not seem to be known what $R<0$ everywhere means in terms of the ergodicity of the system.

The 8- and 16-particle systems were found to have essentially the same curvature statistics, but it remains to be investigated whether systems with particle numbers greater than those studied here by orders of magnitude have the same type of distributions. In particular one would like to know what happens to the fractions of negative curvature and negative Riemann scalar.

Acknowledgments

This study was inspired mainly by the paper 'Some Smooth Ergodic Systems' of Anosov and Sinai (1967) and by the book 'Gravitation' of Misner, Thorne and Wheeler (1973).

I am indebted to the Ahmadu Bello University Computer Center for the use of their CDC Cyber 72.

References

Adler R, Bazin M and Schiffer M 1965 *Introduction to General Relativity* (New York: McGraw–Hill)
Anosov D V 1967 *Proc. Stekhlov Inst. Math.* **90** (Am. Math. Soc. 1969) (Providence (Rhode Island): Am. Math. Soc.)
Anosov D V and Sinai Y G 1967 *Russ. Math. Surveys* **22** 103
Arnol'd V I and Avez A 1968 *Ergodic Problems of Classical Mechanics* (New York: Benjamin)
Balescu R 1975 *Equilibrium and Nonequilibrium Statistical Mechanics* (New York: Wiley)
Barker J A and Henderson D 1976 *Rev. Mod. Phys.* **48** 587
Benettin G, Brambilla R and Galgani L 1977 *Physica* **87**A 381
Bishop R L and Goldberg S I 1968 *Tensor Analysis on Manifolds* (New York: Macmillan)
Brumer P and Duff J W 1976 *J. Chem. Phys.* **65** 3566
Busemann H 1955 *The Geometry of Geodesics* (New York: Academic)
Carnahan B, Luther H A and Wilkes J O 1969 *Applied Numerical Methods* (New York: Wiley)
Chen F F 1974 *Introduction to Plasma Physics* (New York: Plenum)
Copley J R D and Lovesey S W 1975 *Rep. Progr. Phys.* **38** 461
Fröberg C E 1969 *Introduction to Numerical Analysis* 2nd edn (Reading (Mass.): Addison–Wesley)
Goldstein H 1950 *Classical Mechanics* (Reading (Mass.): Addison–Wesley)
Gray D E (ed.) 1957 *American Institute of Physics Handbook* (New York: McGraw–Hill)
Helgason S 1962 *Differential Geometry and Symmetric Spaces* (New York: Academic)
Hénon M and Heiles C 1964 *Astron. J.* **69** 73
Hirsch M W and Smale S 1974 *Differential Equations, Dynamical Systems and Linear Algebra* (New York: Academic)
Misner C W, Thorne K S and Wheeler J A 1973 *Gravitation* (San Francisco: Freeman)
Münster A 1974 *Statistical Thermodynamics* vol 2 (Berlin: Springer)
Toda M 1974 *Phys. Lett.* **48**A 335